**International Journal of Environmental Sciences**
ISSN: 2229-7359
Vol. 11 No. 5, 2025
https://www.theaspd.com/ijes.php

# Environmentally Sustainable Corrosion Control Of Mild Steel Using A Benzene-Based Schiff Base In Hcl Solution

**Shashirekha K.[1,2], B.M. Praveen[1,*], Pavithra M.K.[3], Bharath K. Devendra [4], Manohar R. Rathod[5]**
[1]Department of Chemistry, Srinivas University Institute of Engineering & Technology, Mukka, Karnataka, Mangaluru-574146 India
[1,2]Department of Chemistry, Yenepoya Institute of Technology, Moodabidri, Karnataka, Mangaluru-574225 India
[3]Department of Chemistry, Sahyadri Science College, Vidya Nagar, Shivamogga, Karnataka, Shivamogga -577302 India
[4] Department of Chemistry & Biochemistry, M.S. Ramaiah College of Arts, Science and Commerce (Autonomous), MSR Nagar, MSRIT Post, Bengaluru, Karnataka, 560054, India
[5] Department of Chemistry, Karnatak Science College, Dharwad, Karnataka, 580001, India
Corresponding Author *: bm.praveen@yahoo.co.in

***Abstract***:
*The mild steel (MS) corrosion inhibitive performance of benzene derived Schiff's base in 1 M HCl solution was investigated using weight loss and potentiodynamic polarization measurements. The effect of temperature on the corrosion performance in the presence of inhibitor was evaluated between the range of 303 K and 333 K. The inhibition efficiency was observed to increase with an increase in concentration and temperature. The studied inhibitor follows Langmuir adsorption isotherm by physisorption process. The surface morphological studies of the protective layer on the MS surface specified the adsorption of Schiff's base molecules on metal surface. In the present research, a novel Schiff's base corrosion inhibitor was synthesized, and some quantum chemcial calculations were performed to comprehend the mechanism of inhibition.*
***Keywords:*** *Mild steel, Inhibitor, Schiff's base, EIS, SEM, DFT.*

## INTRODUCTION

In recent years various alloys and metals are used in industry, agricultural, medical and technological purposes. Generally, mild steel is commonly used because of cheap rate, long durability and good mechanical properties (Abiola et al., 2007; Haque et al., 2021; Hebbar et al., 2015). But MS is very much prone to corrosion in acid media. Hence, corrosion control is one of the challenging processes in research area. Huge number of corrosion protection methods are available to inhibit corrosion of metals. Among them, in acid media, usage of corrosion inhibitor is one of the easiest methods to control the corrosion [2-7]. As per literature review, majority of the corrosion inhibitors are organic compounds containing hetero atoms N, S, O in functional groups with hetero cyclic rings. Many of the organic inhibitors are toxic in nature and impart health hazards. To overcome this problem, Schiff's base inhibitor was chosen to control the corrosion.

In this respect, corrosion performance was evaluated by weight loss and potentiodynamic polarization methods. The surface of the inhibited sample was characterized by SEM and FTIR techniques. Besides, in order to provide support for experimental results, quantum chemical parameters were calculated and finally the mechanism of inhibition was proposed.

## MATERIALS AND METHODS:

### Synthesis of 3-(4-hydroxyphenyl)-2-{(E)-[(2E)-3-phenylprop-2-en-1-yliden]amino}propanoic acid

The physico chemical methods were used to synthesize the schiff's base. 3-(4-hydroxyphenyl)-2-{(*E*)-[(2*E*)-3-phenylprop-2-en-1-ylidene]amino}propanoic acid. Analytical grade chemicals and double-distilled water were used for the entire experiments. It is prepared by taking equimolar amount of (1:1) of ethanolic medium of 2-amino-3-(4-hydroxy phenyl) propanoic acid (1g) and (2E)-3phenyl prop-2 enal (1g) in a round bottom flask. The mixture is heated at 303K by adding 30ml of ethanol. An orange/yellowish colored crystal/solid mass thus obtained was purified and filtered through two to three times ethanol washes to

eliminate any remaining reactants and then vacuum-dried. Compound is obtained and utilized for further Characterization studies of 3-(4-hydroxyphenyl)-2-{(E)-[(2E)-3-phenylprop-2-en-1-yliden]amino}propanoic acid.[11]

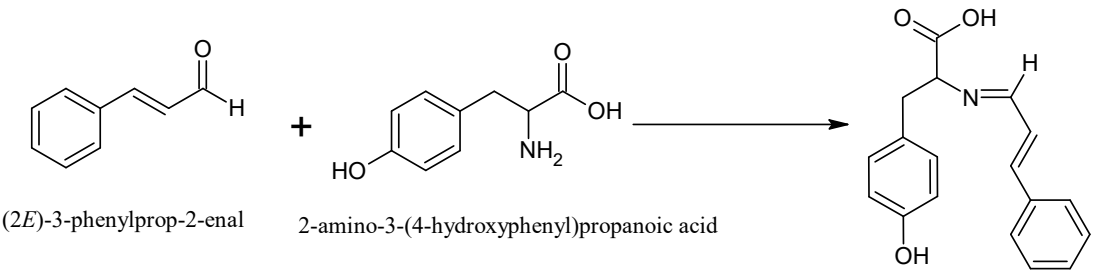


(2*E*)-3-phenylprop-2-enal 2-amino-3-(4-hydroxyphenyl)propanoic acid

3-(4-hydroxyphenyl)-2-{(*E*)-[(2*E*)-3-phenylprop-2-en-1-ylidene]amino}propanoic acid

**FTIR Studies**

The Fourier transform infrared (FTIR) spectrum of the sample is collected using Bruker AlphaP spectrometer.

**Weight loss measurements**

The mild steel sheet (C = 0.2%, Mn = 1.0%, P = 0.25%, S = 0.025% and Rest = Fe) was mechanically press-cut into specimens of dimension 5.0cm × 2.0 cm× 0.1 cm and used for the weightloss studies. Pretreated MS samples were dipped in 100ml 1M HCl solution in the absence and presence of different concentration (10, 20, 30, 40 and 50ppm) of Schiff base at different temperature (303K -333K) for about 2h.

The corrosion rate (CR) of MS was evaluated by using

$CR = \Delta m/St$

where Δm is mass loss,

S is surface area of MS sample

t is immersion time.

**Electrochemical Measurements**

The mild steel sheet (C = 0.2%, Mn = 1.0%, P = 0.25%, S = 0.025% and Rest = Fe) was mechanically press-cut into specimens of dimension 5.0cm × 1 cm × 0.1 cm and used for the electro chemical studies, the working electrode is made of mild steel sheet of same composition immersed in 1M HCl solution.

Electrochemical tests were carried out at room temperature with the help of a ACM instruments electrochemical workstation, provided by ACM Instruments, USA, based in Austin. The three electrodes used in the cell were: steel as the working electrode, platinum as the counter electrode, and an $Hg/Hg_2Cl_2$ electrode as the reference electrode. Before each electrochemical measurement, the working electrode was left in the test solution for 30 minutes to ensure that it had reached the steady-state value of the open circuit potential (OCP). All potentials were recorded relative to the $Hg/Hg_2Cl_2$ electrode [12].

**Surface morphological studies**

SEM images were obtained using a 5.00 kV and 15.kV scanning electron microscope (model: FESEM Carl ZEISS) with a mean large gap of 3.7 mm at different magnifications.

**Quantum mechanical studies**

The quantum chemical parameters are essential to determine the optimized structure for the molecular geometry of the molecules, electronic properties of the molecules and other reactive sites of the molecule. In corrosion inhibition, these parameters are employed to determine possible electron transfer between the inhibitor and metal surface. In the present investigation, the calculation was done by employing Density Functional Theory (DFT).

The quantum mechanical calculations used Becke's three parameter exchange functional for the inhibitor alongside the Lee- Yang-Parr correlation functional with the 6-311 ++ G (d, p) basis set for the

optimization of the molecular geometry of the inhibitor. Gauss View version 6.0 was used for molecular design and visualization, and all computations were done using Gaussian 09 software. This approach allowed for the study of the molecular form and electronic characteristics necessary to comprehend the inhibitor's mechanism of corrosion protection.

## RESULTS AND DISCUSSION:

### FTIR Studies

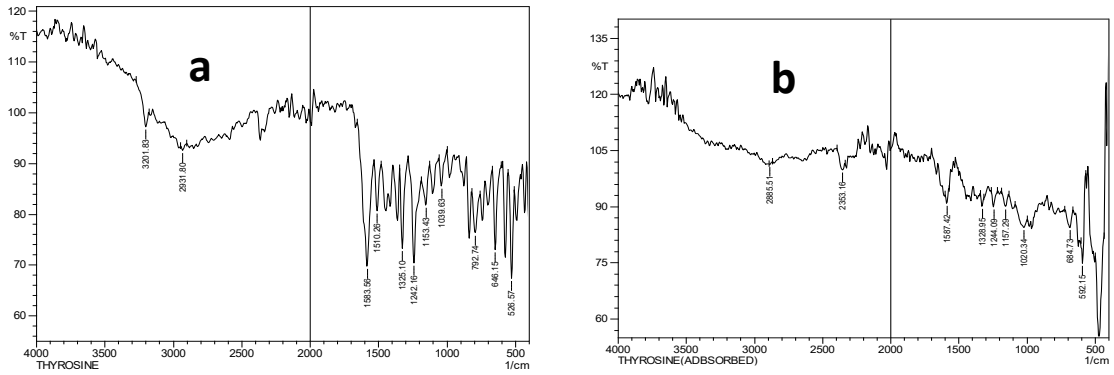


Fig. 2.1. FTIR Graphical representation of Schiff base in a) unabsorbed condition b) adsorbed condition.

Figure2.1a shows the FTIR graphical representation of 3-(4-hydroxyphenyl)-2-{(E)-[(2E)-3-phenylprop-2-en-1-yliden]amino}propanoic acid in unadsorbed condition. Figure 2.1b shows the graphical representation of molecules in adsorbed condition. In Figure 2.1a, NH- peak is observed in 3201cm$^{-1}$ with sp$^2$ CH is obtained in 2931 cm$^{-1}$. CO peak along with C=C aromatic skeletal vibration is obtained in1583cm$^{-1}$. In adsorbed condition, there is an absence of peak in 3201cm$^{-1}$which shows that inhibitor adsorbed on the metal surface through Nitrogen atom.

### Weight loss measurements

Weight loss experiments were performed for MS samples in 1M HCl in the absence and presence of different concentration of Schiff base at different temperature for about 2h. The effect of temperature on corrosion rate of MS in presence of different concentration of Schiff base in 1M HCl is as shown in Figure 2.2.

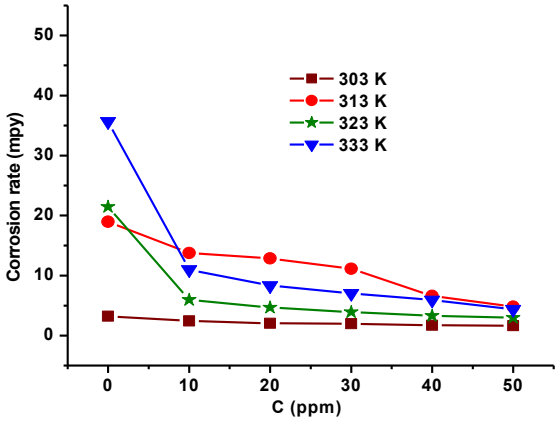


**Fig. 2.2.** Variation in corrosion rate with concentration at different temperature

It is evident from the figure that, the corrosion rate get decreases with increase in concentration at all studied temperature. Moreover, at higher temperature the corrosion rate of mild steel get decreased in presence of inhibitor compared to uninhibited solution.

### Electrochemical Measurements

**Tafel polarization measurement:**

Table 1 lists the electrochemical parameters such as corrosion current density ($i_{corr}$), cathodic Tafel slope ($\beta_c$), anodic Tafel slope ($\beta_a$), and corrosion potential ($E_{corr}$) including inhibition efficiency (IE) based on polarisation studies. The IE was computed using the given relation

$$\%IE = \frac{i^o_{corr} - i_{corr}}{i^o_{corr}} \times 100$$

where $i^o_{corr}$ and $i_{corr}$ are the corrosion current densities in the absence and presence of the corrosion inhibitor, respectively.

Table 1 Electrochemical Tafel results for the corrosion of mild steel in the absence and presence of inhibitor in 1 M HCl in a temperature region of 303–333 K

| **T (K)** | **C (ppm)** | **$E_{corr}$ (V)** | **$i_{corr}$ (mA/cm$^2$)** | **Corrosion rate(mpy)** | **$\beta_a$ (mV/dec)** | **$\beta_c$ (mV/dec)** | **%IE** |
|---|---|---|---|---|---|---|---|
| **303** | Blank | -0.42 | 0.25303 | 2.9326 | 88.2 | 126.3 | - |
| | 10 | -0.362 | 0.19281 | 2.2346 | 97.6 | 122.2 | 23.7995 |
| | 20 | -0.327 | 0.16684 | 1.9221 | 92.3 | 121.1 | 34.063 |
| | 30 | -0.375 | 0.15868 | 1.8391 | 98.2 | 120.3 | 37.2880 |
| | 40 | -0.385 | 0.14421 | 1.6714 | 98.1 | 120.5 | 43.0067 |
| | 50 | -0.375 | 0.13385 | 1.5513 | 97.9 | 124.2 | 47.1011 |
| **313** | Blank | -0.528 | 1.4713 | 17.053 | 76.3 | 126.2 | - |
| | 10 | -0.521 | 1.0477 | 12.142 | 91.4 | 120.3 | 28.79 |
| | 20 | -0.538 | 0.98964 | 11.47 | 92.9 | 121.5 | 32.7370 |
| | 30 | -0.526 | 0.86957 | 10.078 | 95.2 | 124.5 | 40.8978 |
| | 40 | -0.523 | 0.52893 | 6.1303 | 97.1 | 121.9 | 64.0501 |
| | 50 | -0.520 | 0.34092 | 3.9512 | 98.2 | 123.4 | 76.8286 |
| **323** | Blank | -0.358 | 1.5994 | 18.538 | 84.3 | 125.2 | - |
| | 10 | -0.229 | 0.35575 | 4.1231 | 92.4 | 123.1 | 77.7572 |
| | 20 | -0.291 | 0.30741 | 3.5629 | 94.6 | 124.1 | 80.7796 |
| | 30 | -0.345 | 0.25803 | 2.9906 | 96.7 | 122.2 | 83.8670 |
| | 40 | -0.381 | 0.25451 | 2.9497 | 96.9 | 124.2 | 84.0871 |
| | 50 | -0.420 | 0.22126 | 2.5644 | 98.7 | 123.4 | 86.1660 |
| **333** | Blank | -0.522 | 2.8816 | 33.398 | 78.9 | 122.6 | - |
| | 10 | -0.486 | 0.84588 | 9.8038 | 87.6 | 120.6 | 70.7267 |
| | 20 | -0.278 | 0.69141 | 8.0135 | 89.7 | 123.5 | 76.0724 |
| | 30 | -0.487 | 0.56392 | 6.5358 | 94.5 | 122.8 | 80.4844 |
| | 40 | -0.480 | 0.45686 | 5.2951 | 95.2 | 120.7 | 84.1895 |
| | 50 | -0.478 | 0.32258 | 3.7387 | 96.3 | 121.3 | 88.8365 |

International Journal of Environmental Sciences
ISSN: 2229-7359
Vol. 11 No. 5, 2025
https://www.theaspd.com/ijes.php

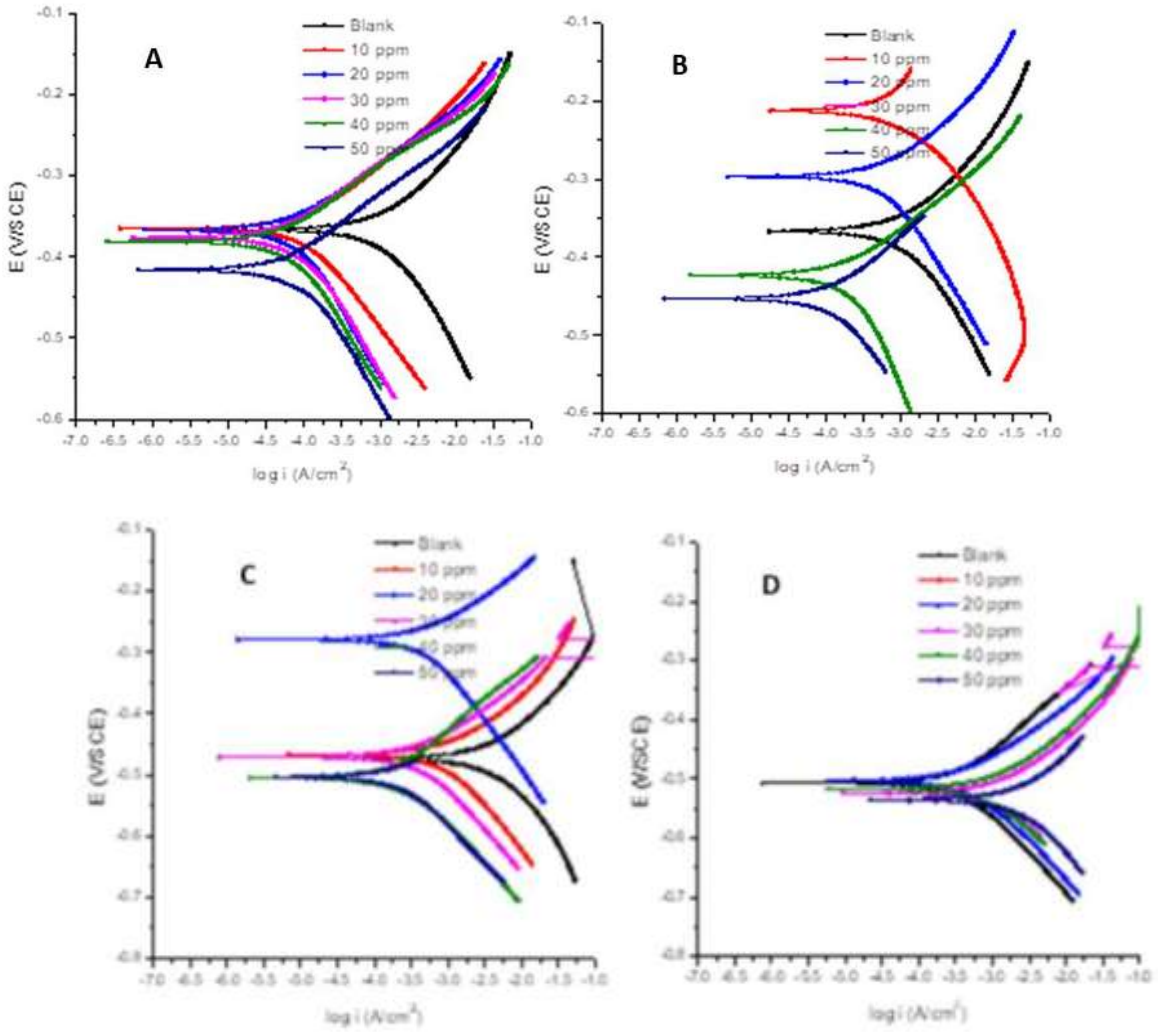


**Fig. 2.3** Tafel plots for mild steel in the absence and presence of inhibitors at different concentrations in 1 M HCl solution at (A) 303 K, (B) 313 K, (C) 323 K and (D) 333 K

Polarisation results illustrates that the corrosion current values get decreases with increasing temperature and it get decreased with increasing concentration of Schiff base at each temperature. It is apparent from the figure 2.3 that, at each temperature there is a variation in both anodic and cathodic branches. This indicate that the inhibitor is involved in inhibiting both anodic and cathodic reactions which is also supported by variation in Tafel slopes given in the table 2.1. In the present study, at all temperature inhibition efficiency get increased with increasing concentration of Schiff base in 1M HCl solution. But protection efficiency is more pronounced at 50 ppm even at 323 and 333K. These results reveal that the studied Schiff base acts as an efficient inhibitor even at elevated temperature.

**Adsorption isotherm**

The interaction of the Schiff base with mild steel surface in 1M HCl can be described by adsorption isotherm at a different temperature range of 303-333 K. The data obtained by Tafel polarisation method is used to determine the extent of electrode surface coverage ($\theta$) given by $\theta$ = %IE/100

The surface coverage values of different concentration at different temperature were fitted with several adsorption isotherms Temkin, Langmuir, Freundlich, Frumkin and flory Huggin's isotherms. But the best fit was obtained with Langmuir adsorption isotherm given by the expression:

$C/\theta = 1/K_{ads} + C$,

International Journal of Environmental Sciences
ISSN: 2229-7359
Vol. 11 No. 5, 2025
https://www.theaspd.com/ijes.php

where $K_{ads}$ represents the equilibrium constant and C denotes the inhibitor concentration. The $K_{ads}$ values were calculated using the straight line that results from plotting $C/\theta$ versus C. the h adsorption plots of Schiff base at different temperature are given in Figure 2.3. From the obtained $K_{ads}$ values, free energy change of adsorption $-\Delta G^0_{ads}$ can be calculated using equation given below

$K_{ads} = (1/55.5) \exp(-\Delta G^0_{ads})/RT$

where 55.5 is the concentration of water in solution, expressed in mol/L, R is the gas constant and T is the absolute temperature.

**Table 2.** Adsorption parameters of Schiff base in 1M HCl at different temperature

| T (K) | $R^2$ | $K_{ads}$ | $-\Delta G^0_{ads}$ (kJ/mol) |
|---|---|---|---|
| 303 | 0.994 | 0.0366 | 1.785 |
| 313 | 0.976 | 0.0346 | 1.698 |
| 323 | 0.999 | 0.5356 | 9.108 |
| 333 | 0.998 | 0.2159 | 6.876 |

The obtained values of $K_{ads}$ and $\Delta G^0_{ads}$ are given in Table 2. the negative values of $\Delta G^0_{ads}$ indicate spontaneous adsorption of studied Schiff base on the MS surface in 1M HCl solution. In general, based on $\Delta G^0_{ads}$ values the type of adsorption of inhibitor molecules on metal surface can be determined. The physisorption is thought to occur when $\Delta G^0_{ads}$ are about −20 kJ/mol or less negative, while chemisorption is occurred when $\Delta G^0_{ads}$ values are around −40 kJ/mol or more negative.

**Fig. 2.3.** Langmuir adsorption isotherm plots of Schiff base at different temperature

However, in the present case, the values of $\Delta G^0_{ads}$ are less negative than −20 kJ/mol which strongly recommends that Schiff's base get absorbed on MS surface by physical adsorption which may be attributed to the presence of N atoms in the molecules.

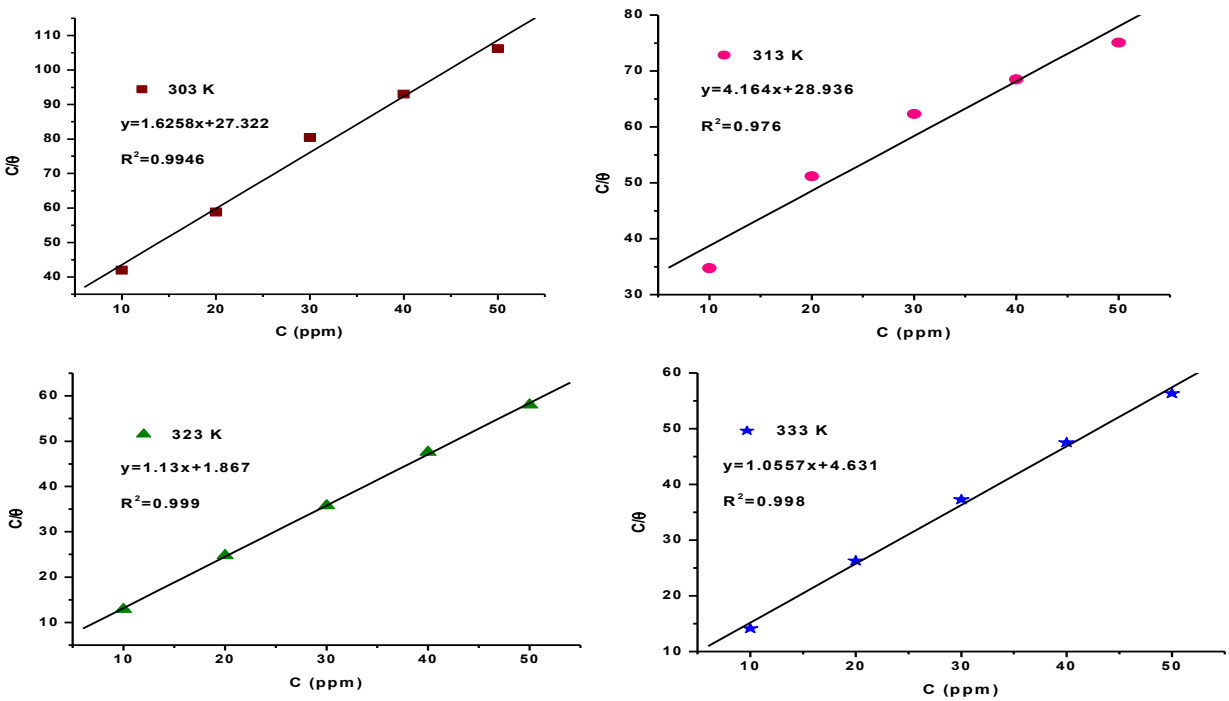


**Scanning Electron Microscopy (SEM) Analysis:**

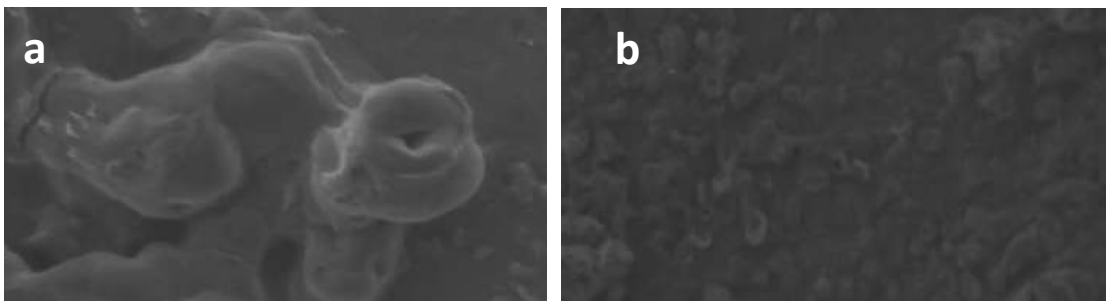

**Fig. 2.4**. SEM images of MS immersed in a) 1M HCl b) 1M HCl +50ppm Schiff base

SEM was used to examine surface of MS that had been submerged in a 1 M HCl solution both without and with 50ppm Schiff base and the respective images are given in **Fig. 2.4**. When the mild steel was submerged in 1 M HCl solution, considerable surface damage was seen (Fig. 2.4(a)), suggesting that the surface is heavily corroded. But in presence of Schiff base, the smooth surface (Fig. 2.4(b)) with decreased roughness was observed on MS surface. This reveals that the inhibitor shield MS surface from corrosion even in the presence of acid. From SEM analysis, it can be concluded that Schiff base acts as good corrosion inhibitor which even prevents corrosion on the MS surface by acting as a protective coating

**Quantum Chemical Calculations**

Molecular orbitals and their properties, like energies, are essential for both chemists and physicists. The frontier molecular orbitals are helpful in identifying the most reactive areas in π-electron systems and elucidating mechanisms of reactions in conjugated molecules. This analysis may better help explain the chemical behavior of molecules if one is concerned with the highest occupied molecular orbital (HOMO) and the lowest unoccupied molecular orbital (LUMO) and their corresponding eigenvalues as well as the gap between them since they greatly influence the stability of a molecule and its process of electron donation and acceptance through electronic transitions.

The newly synthesized Schiff base, 3-(4-hydroxyphenyl)-2-{(E)-[(2E)-3-phenylprop-2-en-1-ylidene]amino}propanoic acid, was fully optimized in its ground state via the computational DFT-B3LYP/ 6-311++G (d, p) method within the Gaussian 09 program. The optimized molecular geometry and dipole moment vectors are presented together with three-dimensional molecular pictures in **Fig.2.5.** Besides, **Fig. 2.6** and **Fig. 2.7** show the calculated molecular orbitals, such as HOMO and LUMO, and the MESP map. These computational details will be used to understand the molecular characteristics and reactivity.

**Global Chemical Reactivity Descriptors: Computational Studies**

For assessing the chemical reactivity and stability of the concerned organic molecule, several global descriptors such as $E_{HOMO}$, $E_{LUMO}$, energy gap (ΔE), chemical potential (μ), electronegativity (χ), chemical softness (S), chemical hardness (η), and electrophilicity (ω) have been computed. These parameters have been computed by using the theoretical standard **equations 1-7** through the energy levels of HOMO and LUMO orbitals.

$$\Delta E = E_{LUMO} - E_{HOMO} \quad (1)$$

$$\chi = \left(\frac{IP + EA}{2}\right) \quad (2)$$

$$\eta = \left(\frac{IP - EA}{2}\right) \quad (3)$$

$$S = \frac{1}{2\eta} \quad (4)$$

$$\omega = \frac{\mu^2}{2\eta} \quad (5)$$

$$\Delta N = \frac{X_{metal} - X_{inh}}{2\,(\eta_{metal} + \eta_{inh})} \quad (6)$$

$$\mu = -\chi \quad (7)$$

**Dipole moment and molecular polarity**

The dipole moment, μ, is one of the most important descriptors of any molecule; higher dipole moments signify greater molecular polarity, which makes the adsorption to charged surfaces more effective, such as a metal substrate used in corrosion inhibition study. The calculated dipole moment of 3.83189 Debye indicates moderate polarity, which allows adsorption onto the metal surface through electrostatic interactions. This property is important in the efficiency of corrosion inhibitors because it determines the strength of molecular interactions with the metallic surface.

HOMO-LUMO gap (ΔE) of 1.18445 eV suggests moderate chemical reactivity and stability. The calculated chemical hardness (η) value of 0.59223 eV suggests a relatively soft molecule and hence higher reactivity through higher electron delocalization. A chemical softness (S) value of 0.29611 eV further suggests the high polarizability of the molecule.

The electrophilicity index (ω) of 13.2487 eV suggests that the molecule possesses a strong electrophilic character and hence high reactivity towards nucleophiles. Furthermore, the chemical potential (μ) value of -3.96137 eV suggests that the studied compound is stable and non-decomposable.

**Analysis of HOMO, LUMO, and ΔN**

The highest occupied molecular orbital (HOMO) and lowest unoccupied molecular orbital (LUMO) energy levels are good molecular reactivity indicators. The energy level of the HOMO (-4.55359 eV) suggests the donating ability of the molecule, and the energy level of the LUMO (-3.36914 eV) suggests its accepting ability. The relatively small HOMO-LUMO gap (ΔE = 1.18445 eV) suggests the moderately reactive nature of the studied compound with the possibility of an electron transfer process.

The portion of the transferred electrons (ΔN) of 2.56543 obtained was calculated. The ΔN value, according to Lukovits' analysis, suggests the donor nature of the electrons from the inhibitor molecule towards the metal surface. A ΔN value of less than 3.6 suggests an enhanced ability of the metal surface for electron acceptance and hence improved inhibition efficiency of the studied compound. This further suggests that the inhibitor is able to donate the charge to the metal and can shield it through the formation of an effective protective coating against corrosion. The ΔN value obtained suggests the high potential of the adsorption of the compound, supporting further its efficiency as a corrosion inhibitor.

**Table 2.3** DFT parameters of the studied inhibitor

| **Parameter** | 3-(4-hydroxyphenyl)-2-{(E)-[(2E)-3-phenylprop-2-en-1-ylidene]amino}propanoic acid **(eV)** |
|---|---|
| $E_{HOMO}$ | -4.55359 |
| $E_{LUMO}$ | -3.36914 |
| ΔE | 1.18445 |
| Dipole moment | 3.83189 |
| Ionization potential (IP) | 4.55359 |
| Electron affinity (EA) | 3.36914 |

| | |
|---|---|
| Electronegativity (χ) | 3.96137 |
| Chemical potential (μ) | -3.96137 |
| Chemical hardness (η) | 0.59223 |
| Chemical softness (S) | 0.29611 |
| Electrophilicity (ω) | 13.2487 |
| ΔN | 2.56543 |

**Molecular electrostatic potential (MESP) analysis**

The Molecular Electrostatic Potential (MESP) map is a visual representation of the charge distribution within the molecule, which delineates areas prone to electrophilic and nucleophilic interactions. **Fig. 2.7** is the MESP surface of the target compound, where red coloration represents electron-rich areas (nucleophilic centers) and blue coloration represents electron-deficient areas (electrophilic centers). The oxygen atoms of the hydroxyl (-OH) and carboxyl (-COOH) functional groups exhibit high negative electrostatic potential, representing strong nucleophilic activity, while the nitrogen atom of the Schiff base moiety is a major electrophilic site.

These findings advance our understanding of the structural and electronic characteristics of the target organic molecule, to the advantage of its potential applications in material science and pharmaceutical research.

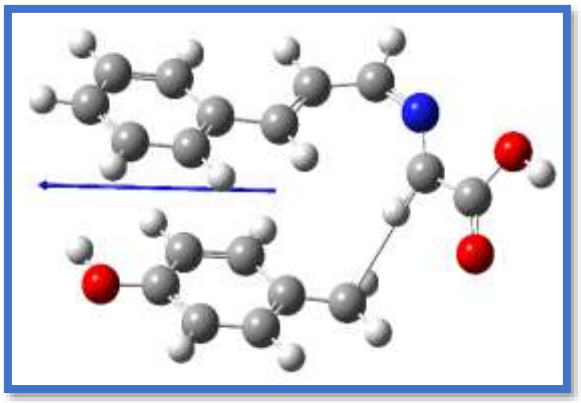

**Fig. 2.5.** Computed ground-state molecular geometries and dipole moment orientations of molecule 3-(4-hydroxyphenyl)-2-{(E)-[(2E)-3-phenylprop-2-en-1-ylidene]amino}propanoic acid obtained through B3LYP/6–311++G (d, p) methodology

**Fig. 2.6** 3-D depictions of the optimized structure, HOMO and LUMO orbitals, along with their energy levels, for 3-(4-hydroxyphenyl)-2-{(E)-[(2E)-3-phenylprop-2-en-1-ylidene] amino} propanoic acid

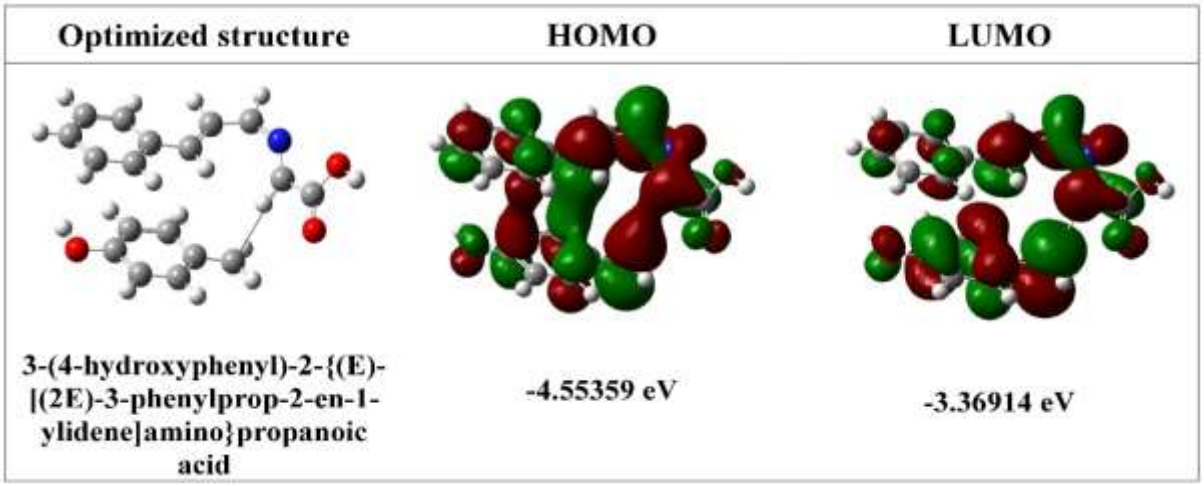

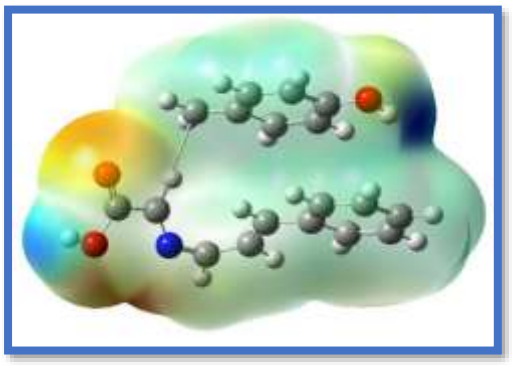

**Fig.2.7.** Three-dimensional molecular electrostatic potential (MESP) graphs for molecule 3-(4-hydroxyphenyl)-2-{(E)-[(2E)-3-phenylprop-2-en-1-ylidene] amino} propanoic acid

## CONCLUSION:

The studied Schiff base was found to be an effective corrosion inhibitor for mild steel in 1M HCl even at elevated temperatures. Schiff base shows nearly 89% protection efficiency at 50 ppm concentration at 323 K and it shows good inhibition property even at 333K. The experimental results obtained from weightless experiments are in good agreement with Tafel polarisation method. The adsorption of Schiff base follows Langmuir adsorption isotherm via physisorption mechanism. The findings of quantum chemical calculations explain the efficacy of inhibitor is due to the presence of the oxygen atoms of the hydroxyl (-OH) and carboxyl (-COOH) functional groups along with nitrogen atom of the Schiff base moiety.

**REFERENCES:**

[1] Abiola, O. K., Oforka, N. C., Ebenso, E. E., & Nwinuka, N. M. (2007). Eco-friendly corrosion inhibitors: the inhibitive action of Delonix Regia extract for the corrosion of aluminium in acidic media. Anti-Corrosion Methods and Materials, 54(4), 219-224. https://doi.org/10.1108/00035590710762357
[2] Arab, S. T., & Noor, E. A. (1993). Inhibition of acid corrosion of steel by some S-alkylisothiouronium iodides. Corrosion, 49(2), 122-129. https://doi.org/10.5006/1.3299206
[3] Luo, H., Guan, Y. C., & Han, K. N. (1998). Corrosion inhibition of a mild steel by aniline and alkylamines in acidic solutions. Corrosion, 54(9), 721-731. https://doi.org/10.5006/1.3284891
[4] Mert, M. E., Güngör, C., & Mert, B. D. (2025). Analytical study on mild steel corrosion inhibition in acidic environment: DFT modeling and RSM optimization. Fuel, 381, 133729. https://doi.org/10.1016/j.fuel.2024.133729
[5] Lagrenee, M., Mernari, B., Chaibi, N., Traisnel, M., Vezin, H., & Bentiss, F. (2001). Investigation of the inhibitive effect of substituted oxadiazoles on the corrosion of mild steel in HCl medium. Corrosion science, 43(5), 951-962. https://doi.org/10.1016/S0010-938X(00)00076-7
[6] Kumar, R., Chopra, R., & Singh, G. (2017). Electrochemical, morphological and theoretical insights of a new environmentally benign organic inhibitor for mild steel corrosion in acidic media. Journal of Molecular Liquids, 241, 9-19. https://doi.org/10.1016/j.molliq.2017.05.130
[7] Bentiss, F., Traisnel, M., & Lagrenee, M. (2000). The substituted 1, 3, 4-oxadiazoles: a new class of corrosion inhibitors of mild steel in acidic media. Corrosion science, 42(1), 127-146. https://doi.org/10.1016/S0010-938X(99)00049-9
[8] Praveen, B. M., Chakravarthy, A. J., Prasanna, B. M., Devendra, B. K., & Pavithra, M. K. (2025). Author Correction: Experimental and theoretical investigation of cyclohexanone derivative (CHD) as a corrosion inhibitor for mild steel in 1 M HCl. Scientific Reports, 15, 14527. https://doi.org/10.1038/s41598-025-99217-z
[9] Lagrenee, M., Mernari, B., Chaibi, N., Traisnel, M., Vezin, H., & Bentiss, F. (2001). Investigation of the inhibitive effect of substituted oxadiazoles on the corrosion of mild steel in HCl medium. Corrosion science, 43(5), 951-962. https://doi.org/10.1016/S0010-938X(00)00076-7
[10] Shwetha, K. M., Praveen, B. M., Devendra, B. K., Saleh, D. I., & Rathod, M. R. (2025). Investigations of a new derivative as an effective mild steel corrosion inhibitor in acidic medium using experimental, electrochemical and DFT simulation methods. Inorganic Chemistry Communications, 177, 114289. https://doi.org/10.1016/j.inoche.2025.114289
[11] F. Bentiss, M. Traisnel, L. Gengembre, M. LagrenéeInhibition of acidiccorrosion of mild steel by 3,5-diphenyl-4H-1,2,4-triazoleAppl. Surf. Sci., 161 (2000), pp. 194-202
[12] Rathod, M. R., Rajappa, S. K., Praveen, B. M., & Bharath, D. K. (2021). Investigation of Dolichandra unguis-cati leaves extract as a corrosion inhibitor for mild steel in acid medium. Current Research in Green and Sustainable Chemistry, 4, 100113. https://doi.org/10.1016/j.crgsc.2021.100113